Onboard Flow Sensing for Rotary-Wing UAV Pitch Control in Wind

Derrick W. Yeo,* Nitin Sydney† and Derek A. Paley ‡
University of Maryland, College Park, Maryland, MD 20742, U.S.A

Due to their size, small rotorcraft are vulnerable to external flow disturbances that are challenging to flight stability and control. This paper describes preliminary results from using onboard flow measurements to augment inertial sensors for attitude control. We derive a dynamic model that captures the aerodynamic effects of wind on a single degree-of-freedom tandem-rotor test stand. A pair of rotors generate control moments through differential thrust, subject to wind-induced effects such as blade-flapping and induced thrust. We design an attitude-control strategy that uses airspeed measurements to feedback linearize the system in the presence of an edgewise flow. Low-speed wind tunnel tests provide empirical coefficients to model the flow-induced moments and thrust generation for a small, stiff rotor. A test stand equipped with an inertial measurement unit and airspeed probe demonstrates the use of onboard flow-sensing for attitude stabilization via feedback control in wind.

Nomenclature

$\mathbf{e}_1, \mathbf{e}_2, \mathbf{e}_2$	Unit vectors in the inertial reference frame
$\mathbf{b}_1, \mathbf{b}_2, \mathbf{b}_2$	Unit vectors in the body reference frame
I	Carriage planar moment of inertia
$\mathbf{h}_O$	Angular momentum of the test stand
$\mathbf{M}_O$	Moment about the origin
θ	Carriage pitch angle
α	Rotor flap angle
V_∞	Freestream velocity
Ω	Rotor rotation rate
v	Rotor induced velocity
T	Rotor thrust vector
S	Rotor moment due to flapping
$k_T^{(1)}$,$k_T^{(2)}$	Rotor thrust coefficients
k_f,k_s	Rotor flap coefficients
l	Lateral distance between rotor and pivot
d	Vertical distance between rotor and pivot
u	Control input
K	Control gain matrix
Subscript	
i	Rotor index

*Assistant Research Scientist,Department of Aerospace Engineering Department, AIAA Member.
†Systems Engineer,Mitre Corporation, AIAA Student Member.
‡Willis H. Young Jr. Associate Professor of Aerospace Engineering Education, Department of Aerospace Engineering and the Institute for Systems Research, AIAA Senior Member.

I. Introduction

Small, unmanned rotary-wing vehicles have recently begun serving a wide variety of purposes in the public domain, but their low mass leaves them particularly susceptible to disturbances from wind and other external flow effects like gusts. Multi-rotor helicopters use independent rotors to provide lift and control moments, providing researchers with mechanically simple and effective vertical-flight platforms. Typically, the lift and resultant torque due to each rotor is approximated with simple aerodynamic models developed around hover conditions. Although these models have proven adequate in low advance-ratio flight conditions,[1] they may not account for the flow conditions associated with high-speed forward flight or the effects of external flow sources. This work investigates the use of onboard, spatially distributed flow sensing as a means to augment the traditional inertial-sensing and control paradigm. Real-time measurements of the flow field around a flying vehicle provide a description of ambient conditions that may not be observable by inertial-based instruments.

The contributions of the research described in this paper are (1) a single-degree-of-freedom dynamic model that includes the aerodynamic effects of an edgewise free-stream on a rotor; (2) a nonlinear feedback control law that features the use of onboard flow measurements to generate estimates of the wind for feedback linearization; and (3) results from ongoing experimental validation using a test stand instrumented with a multihole airspeed probe. The outline of the paper is as follows. Section II provides background of small rotorcraft control and onboard flow sensing is provided in. Section III describes the dynamic model and control design. Section IV presents preliminary results from a single degree-of-freedom test stand, and Section V summarizes the paper and ongoing work.

II. Background

In contrast to natural flyers that rely on flow sensors for flight control,[2,3] small UAS instrumentation is focused on inertial measurements. Conventional flow probes providing air-data measurements such as airspeed, angle-of-attack, and side-slip angle have been successful in applications involving conventional fixed-wing flight within the traditional flight envelope[4–6] and for turbulence mitigation.[7] These platforms provide a baseline capability for more advanced tests in areas such as cooperative control[8] for both fixed-wing and rotary-wing vehicles.[9,10]

At the path-planning level, onboard flow sensing provides information that can drive vehicle configuration or guidance decisions based on flight conditions. For example, Cox et al.[11] used pressure-based estimates of the lift curve above an airfoil as feedback for an automated cruise flap. Yeo et al.[12] used real time stall detection through pressure sensing to change controller modes on a small, fixed-wing UAV during transition between forward flight and propeller-borne hover. In earlier work,[13] the authors demonstrated the use of onboard flow sensing by using distributed flow measurements to detect and avoid the downwash of a second rotary wing UAV.

This paper seeks to augment inertial-based attitude-control strategies with onboard flow sensing. External wind information is provided by a novel probe-based flow-measurement package. Unlike traditional measurement techniques employed on small rotors such as hot-wire anemometry[14] and optical velocimetry methods,[11,15,16] the pressure-probe-based approach used here is inherently portable, rugged and well-suited for use onboard small UAVs. The instrumentation system is capable of providing flow speed measurements above 0.3 m/s in real time,[13] which is below the noise floor of comparable pitot-static probes. This low-speed measurement capability enables the implementation of flow-based guidance and control. Additional flow information across the rotors promises to improve quadrotor stabilization in wind. Sydney et al.[17] formulated a simulation model and controller using feedback linearization, demonstrating the potential for using onboard sensing for improved attitude control in an estimated wind field .

Rotors in an edgewise flow are subject to aerodynamic effects[18,19] not frequently modeled on small UAVs. Blade flap and induced-thrust effects are not commonly encountered in indoor flight, which generally involves low advance-ratio conditions.[20–22] However, these aerodynamic effects pose significant challenges to small quadrotors in outdoor environments. Hoffman et al. demonstrate that even moderate translational speeds can challenge attitude and altitude control.[23] They also note that, while the integrator term in a linear controller offers a small degree of moment compensation in forward flight, it must adapt rapidly as conditions change, in order to accommodate unmodelled effects. In subsequent work, Huang et al.[24] implemented control compensation for the moments generated by translational velocity and aircraft pitch

angle. Their work focused on mitigating the aerodynamic effects from forward flight, and a pre-calculated look-up table of thrust produced under different wind conditions proved effective when the relative wind vector was self-generated through vehicle motion. Their approach relies on ground-speed estimates and does not fully account for the aerodynamic disturbances due to unknown wind.[25] Pounds et al.[26] showed that some of the flap moments may also be alleviated on a quadrotor using a custom-built, teetering-hub system which represents a relatively significant increase in mechanical complexity for small multirotors.

The work described below is unique in how flow feedback is used to estimate instantaneous wind conditions and compensate for the resulting aerodynamic moments on a rotor carriage. Ground-based testing demonstrates how sensing and control elements are implemented in a controlled flow environment. The paper presents a dynamic model that accounts for the aerodynamic effects of wind on a tandem-rotor pitch stand, and a control that uses onboard airspeed measurements for feedback linearization of the dynamics.

III. Test Stand Pitch Dynamics and Control

A. Pitch Dynamics

We start by introducing two reference frames. See Fig. 1 for a sketch of the test stand with the relevant forces and reference frames. Let $\mathcal{I} = \{O, \mathbf{e}_1, \mathbf{e}_2, \mathbf{e}_3\}$ be an inertial reference frame with origin O located at the pivot point. There is also a body-fixed frame $\mathcal{B} = \{O, \mathbf{b}_1, \mathbf{b}_2, \mathbf{b}_3\}$ attached to the test stand at O. Frame $\mathcal{B}$ is centered at the pivot point with the $\hat{\mathbf{b}}_1$ axis along the bar and the $\hat{\mathbf{b}}_3$ axis aligned with the propellor attachment rods. Due to blade flapping, the rotation plane of rotor i is tilted from $\mathbf{b}_1$ by its corresponding flap angle α_i, where $i = 1, 2$.

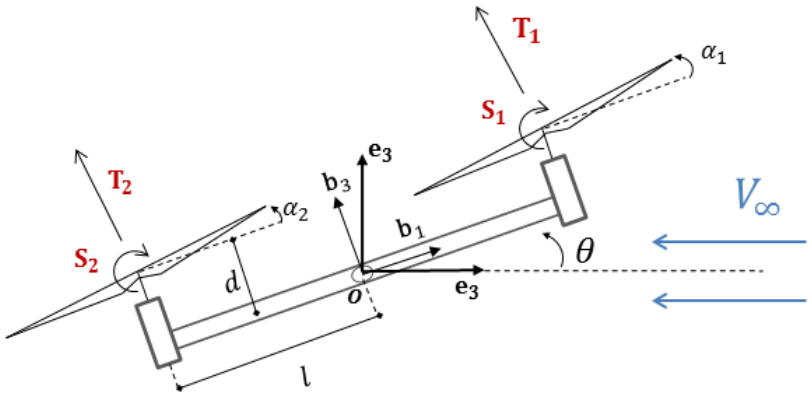

Figure 1: Free-body diagram of pitch stand system

Figure 1 shows a free body diagram of the system, where $\mathbf{T}_1$ and $\mathbf{T}_2$ are the thrust forces from the propellors, and $\mathbf{S}_1$ and $\mathbf{S}_2$ are moments induced on the stand by the rotors due to blade flapping. The dynamics of the test stand are determined through the angular momentum relation

$$\frac{^{\mathcal{I}}d}{dt}\mathbf{h}_O = \mathbf{M}_O, \tag{1}$$

where $\mathbf{h}_O$ is the total angular momentum about O and $\mathbf{M}_O$ is the total external moment acting about O. Let I be the planar moment of inertia of the test stand about O. The out-of-plane component of the angular momentum is

$$\mathbf{h}_O = -I\dot{\theta}\mathbf{b}_2, \tag{2}$$

where $\dot{\theta}$ is the pitch rate. Note that the rotors spin in opposite directions, though we take these rotation rates to be $\Omega_1 > 0$ and $\Omega_2 > 0$. The pitch equation of motion is

$$-I\ddot{\theta} = M_2. \tag{3}$$

There are two moments acting on the vehicle from each rotor: a moment M_T due to thrust and a pure torque M_S caused by the structural flexing of the blades due to blade flap, so

$$M_2 = M_T + M_S. \tag{4}$$

First consider the moment due to the thrust from each rotor, accounting for the tilt in the rotor plane due to flapping, is

$$M_T = -T_1(l\cos\alpha_1 + d\sin\alpha_1) + T_2(l\cos\alpha_2 - d\sin\alpha_2). \tag{5}$$

The thrust generated by each propellor is affected by the flow conditions into the rotor plane due to relative climb/descent and forward velocity. For each rotor, blade elemement momentum theory gives[18]

$$T_i = k_T^{(1)}\Omega_i^2 - k_T^{(2)}(w_i + v_i)\Omega_i, \tag{6}$$

where v_i is the induced velocity generated by the i^{th} rotor and w_i is the local flow velocity into rotor i due to body motion and external wind. (The rotor characteristics $k_T^{(1)}$, $k_T^{(2)}$, and v for a given rotation rate are found empirically.) Let V_∞ be the magnitude of the freestream velocity along the $-e_1$ direction (see Fig. 1); the flow speed through each rotor is

$$w_1 = V_\infty \sin(\theta + \alpha_1) + l\dot{\theta} \tag{7}$$

$$w_2 = V_\infty \sin(\theta + \alpha_2) - l\dot{\theta}. \tag{8}$$

The flapping moment M_S arises from the structural loads applied to the rotor shafts through the propeller hubs. Note that this moment always acts to tilt a rotor away from the incoming flow, regardless of which way the rotor is spinning, hence

$$M_S = -(S_1 + S_2). \tag{9}$$

Assuming stiff hubs such as those found on small multi-rotors, the moment transmitted through the blades is assumed to be proportional to the flap angle α and the square of Ω,[19] i.e.,

$$S_i = k_S\Omega_i^2\alpha_i. \tag{10}$$

The flap angle α_i is proportional to the component of the relative wind parallel to the rotor plane, following Hoffman et al.[24] The downstream rotor encounters a different in-plane velocity due to the wake of the upstream rotor. This paper models the effect by adding the $\mathbf{b}_1$ component of the induced velocity generated by the upstream rotor. For $|\theta| \leq \dfrac{\pi}{2}$, the flap angles are computed using

$$\alpha_1 = k_f(V_\infty \cos\theta) \tag{11}$$

$$\alpha_2 = k_f(V_\infty \cos\theta - v_1 \sin\alpha_1). \tag{12}$$

Substituting Eqs.(4) – (12) into Eq.(3) and rearranging yields the equation of motion

$$\begin{aligned}\ddot{\theta} = -\frac{1}{I}\Big[&-(k_T^{(1)}\Omega_1^2 - k_T^{(2)}(w_1 + v_1)\Omega_1)(l\cos\alpha_1 + d\sin\alpha_1) + \\ &(k_T^{(1)}\Omega_2^2 - k_T^{(2)}(w_2 + v_2)\Omega_2)(l\cos\alpha_2 - d\sin\alpha_2) - k_S\Omega_1^2\alpha_1 - k_S\Omega_2^2\alpha_2\Big].\end{aligned} \tag{13}$$

B. Control Design

To design a state-space controller, Eq.(13) is put in state-space form and simplified. Assume both rotors are subject to the same free stream and flap at the same angle (i.e., $\alpha = \alpha_1 = \alpha_2$) (we do not measure the flow over each rotor separately); Flap angle α is

$$\alpha = k_f(V_\infty \cos\theta). \tag{14}$$

With $d \ll l$ and a small-angle approximation of α ($\cos\alpha \approx 1$ and $\sin\alpha \approx \alpha$), Eq.(13) reduces to

$$\begin{aligned}\ddot{\theta} &= -\frac{1}{I}\Big[-(k_T^{(1)}\Omega_1^2 - k_T^{(2)}(V_\infty \sin(\theta+\alpha) + l\dot{\theta} + v_1)\Omega_1)l + \\ &\quad (k_T^{(1)}\Omega_2^2 - k_T^{(2)}(V_\infty \sin(\theta+\alpha) - l\dot{\theta} + v_2)\Omega_2)l - k_S\Omega_1^2\alpha - k_S\Omega_2^2\alpha\Big]. \end{aligned}\tag{15}$$

Now let $\Omega_1 = \Omega + u$ and $\Omega_2 = \Omega - u$, which reduces the number of controls to one from two (the individual rotation rates of the propellers). The differential rotation rate u augments the hover rotation rate Ω. The corresponding induced velocity $v_1 = v_2 = v$ is measured offline. Consequently the equation of motion becomes

$$\ddot{\theta} = -\frac{1}{I}\left[-4lk_T^{(1)}\Omega u + lk_T^{(2)}\Omega 2l\dot{\theta} + 2lk_T^{(2)}[V_\infty \sin(x_1+\alpha) + v]u - 2k_S\alpha\Omega^2 - 2k_S\alpha u^2\right] \tag{16}$$

Equation (16) is further simplified by considering the hover condition. Assume rotation rates are small and neglect the damping term associated with rotation rate $\dot{\theta}$. Also assume that the differential rotor inputs required to generate control moments are small compared to the hover rotation rate, i.e., $\mathcal{O}(u) \ll \mathcal{O}(\Omega)$ and $\mathcal{O}(u) \ll \mathcal{O}(\Omega u)$. Let $[x_1, x_2, x_3]^\intercal = [\int_0^t \theta \mathrm{d}t, \theta, \dot{\theta}]^\intercal$. In state-space form, using Eq.(14), the equations of motion are

$$\dot{x}_1 = x_2 \tag{17}$$

$$\dot{x}_2 = x_3 \tag{18}$$

$$\dot{x}_3 = -\frac{1}{I}[-4lk_T^{(1)}\Omega u - 2k_S\Omega^2 k_f V_\infty \cos x_2] + \mathcal{O}(u). \tag{19}$$

The feedback control

$$u = -\frac{k_S k_f \Omega V_\infty \cos x_2}{2k_T^{(1)} l} + \frac{\nu}{\frac{4}{I}k_T^{(1)} l\Omega}. \tag{20}$$

linearizes the system (17)–(19) using onboard measurements of $V_\infty \cos x_1$. The feedback-linearized equations of motion are

$$\dot{x}_1 = x_2 \tag{21}$$

$$\dot{x}_2 = x_3 \tag{22}$$

$$\dot{x}_3 = \nu, \tag{23}$$

where the choice $\nu = -Kx$ exponentially stabilizes the origin of the system. (Note, to stabilize a non-zero pitch θ_{des}, we change coordinates to $x' = x + [0, \theta_{des}, 0]^\intercal$)

C. Simulation Results

To test the flow-feedback linearization strategy, the controller designed in Section V was simulated with the airspeed estimated using a recursive Bayesian filter.[27] Assume the wind direction is known and the wind magnitude is estimated. Figure 2(a) shows a stable equilibrium where both rotors are pointed directly away from the incoming flow. Figure 2(b) plots the open-loop response of the system when it is initialized at $\theta = 0$ and converges to equilibrium at $\theta = \pi/2$.

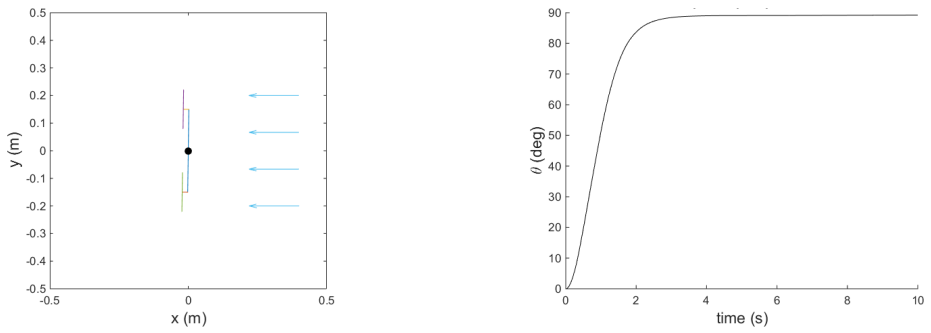

(a) Equilibrium point (b) Open-loop response

Figure 2: Simulated open-loop response of the system to steady wind

Figure 3 shows the response of the closed-loop system using the nonlinear controller (20). The system reaches the desired angle $\theta = -\pi/6$ from an initial condition of $\theta = \pi/6$. At each flow condition, the feedback-linearizing term may be removed for comparison by setting the airspeed measurement to zero. Figure 3(a) shows little benefit of flow compensation in hover, where simulated measurement noise causes steady state error. Figure 3(b) demonstrates the advantage of flow feedback at a freestream velocity of 1.5m/s.

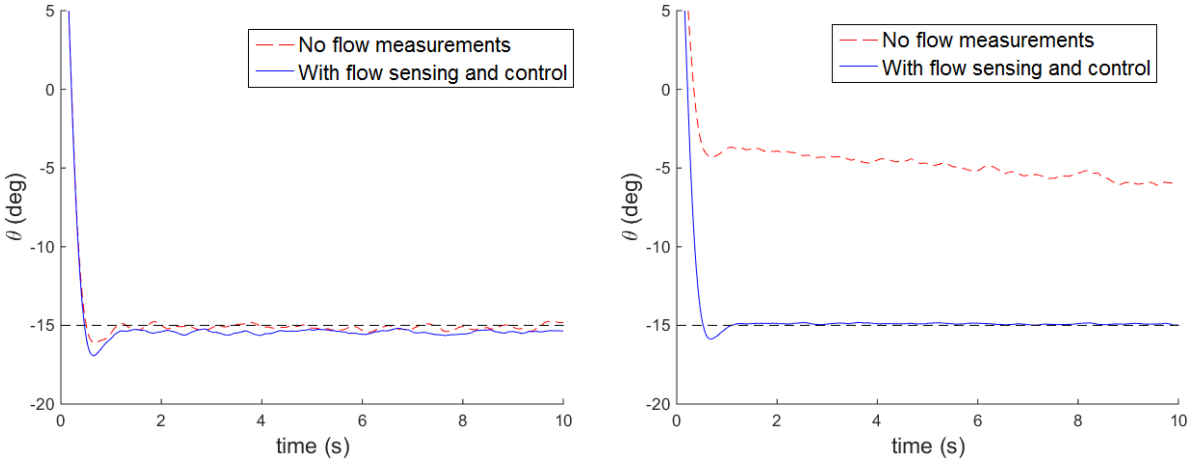

(a) Hover (no wind) (b) 1.5m/s freestream

Figure 3: Simulated closed-loop results in hover and a 1.5m/s freestream

IV. Experimental Methodology and Results

We built a single degree-of-freedom test stand to experimentally evaluate the proposed controller (20). A set of 130mm plastic rotors were characterized using wind-tunnel experiments and incorporated in the test stand. This section presents the characterization of the rotors and experimental results.

A. Rotor Characterization

A WLToys V949 rotor system was mounted on an ATI-IA Nano 17 Force Torque (FT) transducer and tested at a number of freestream velocities. Six-axis force and torque measurements were taken at 1kHz by an Athena II PC104 embedded computer. An integrated optical encoder system provided closed-loop RPM control and measurements during the tests. The flow field was generated by the UMD educational open-jet wind tunnel, and airspeed measurements were taken using a hot-wire anemometer. Fig. 4 shows the prototype rotor test stand; Fig. 5 presents sample data from a V949 rotor.

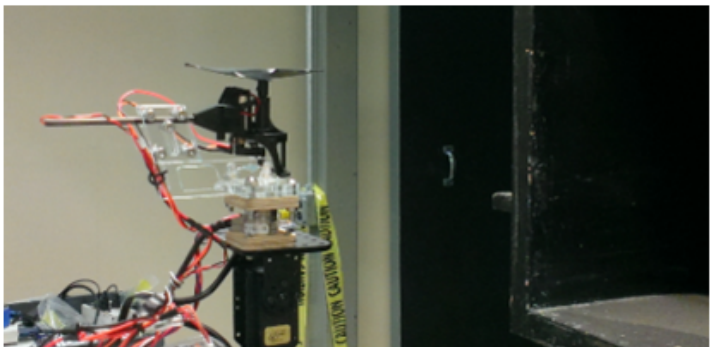

Figure 4: Rotor test stand

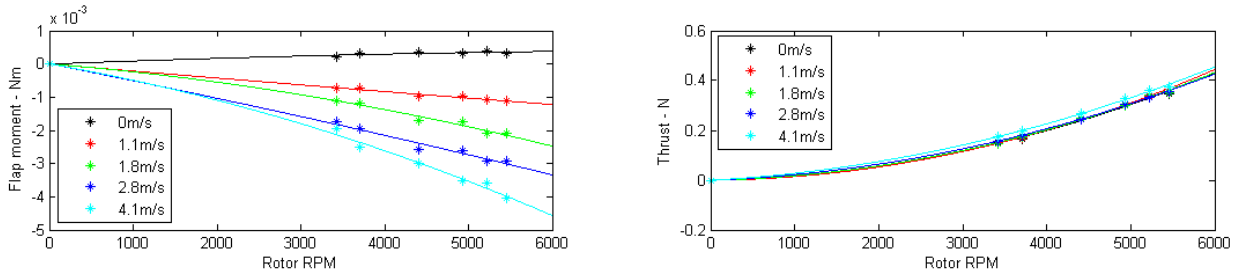

Figure 5: V949 rotor test results

Test data shows the flap moments generated by a V949 rotor are comparable in magnitude to rotor torque, even in moderate freestream velocities. As instrumentation to measure blade flap deflection is still being developed, we seek the product of the flap-moment coefficients $k_S k_f$ used in Eqs. (9) and (11). Hover data provides $k_T^{(1)}$ and $k_T^{(2)}$ used in Eq.(6) through a quadratic fit. Finally, the induced velocity v for a given Ω may be calcuated using thrust data and momentum theory[18] from

$$T_k = 2\rho A v_k (w_k + v_k). \tag{24}$$

A list of experimental and simulated parameters are shown in Table 1.

B. Single-Degree-of-Freedom Stand

A set of V949 rotors and drive assemblies were used to build a test stand. The carriage is supported on plastic bushings and is free to rotate in pitch. It carries an IMU for attitude measurements and a custom-built airspeed probe to measure velocity measurements along the rotor plane. The probe uses a pair of opposite-facing pressure ports to measure differential pressure along an axis, which is used to calculate the velocity component of the flow. More details on the design and calibration of these probes is available.[13] The probe is aligned with $\mathbf{b}_1$ and measures $V_\infty \cos\theta$ in Eq. (11).

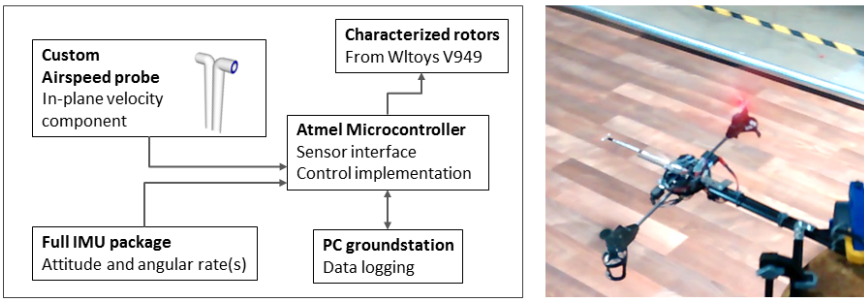

Figure 6: 1DOF pitch stand

The nonlinear control designed in Section III was implemented on a micro-controller. The gain matrix K is tuned for hover. Measurements from the airspeed probe are filtered and used to compute the flow compensation term. The simulated test cases were reproduced and the carriage attempts to stabilize to $\theta = -15°$ when initialized at $\theta = 15°$. Results from the prototype test carriage in hover and in a 1.5 m/s free stream are shown in Fig. 7(a) and Fig. 7(b), respectively. At each condition, the effect of flow feedback was evaluated by setting the velocity measurement to zero.

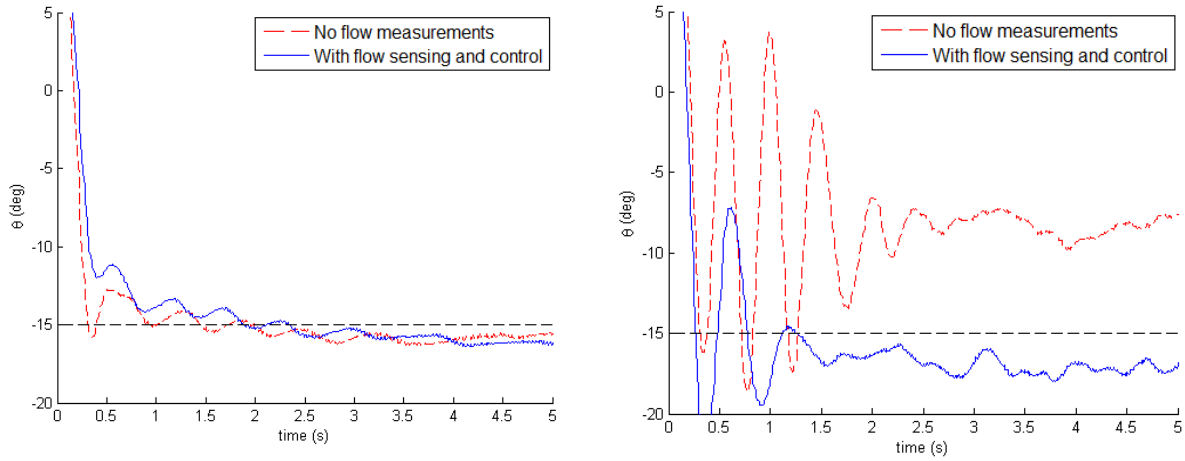

(a) Hover (no wind)

(b) 1.5m/s freestream

Figure 7: Experimental results at hover and in a 1.5m/s freestream

Without flow feedback, the system responds poorly in a 1.5m/s free stream with large pitch oscillations before settling to a steady state error of approximately $+7°$. This indicates that without feedback, the moments caused by the freestream represent a significant challenge to a flight controller. With flow compensation enabled, the carriage undergoes fewer oscillations and settles to a steady state error of approximately $-3°$. Note that feedback overcompensates for the flow-induced moment. In both cases, the experimental results shows more oscillatory behavior than the simulations. We believe this behavior is due to unmodelled effects present on the prototype stand (such as friction) and a slow control loop which limits the magnitude of the control gain K.

C. Gust Mitigation Results

Flow-sensing feedback control could provide gust rejection capabilities by using onboard measurements to react rapidly to changing wind conditions. We tested the proposed controller in a gust mitigation scenario to experimentally evaluate its ability to maintain a reference pitch angle in a varying freestream.

A gust-generation system was built using a bank of Dyson blower-style fans to create a turbulent

freestream with a small cross-flow velocity component. In these tests, a rapid 0m/s to 2.5m/s increase in freestream velocity was realized using a set of servo-actuated shutters. We implemented the feedback control scheme on an improved version of the test stand and ran experiments in which the carriage attempts to maintain $\theta = 0°$ despite changing flow conditions. The test was first run without flow measurements in the controller and then repeated with flow-feedback enabled. Pitch angle and airspeed measurement histories from the two test cases are compared in Fig. 8(a) and Fig. 8(b), respectively.

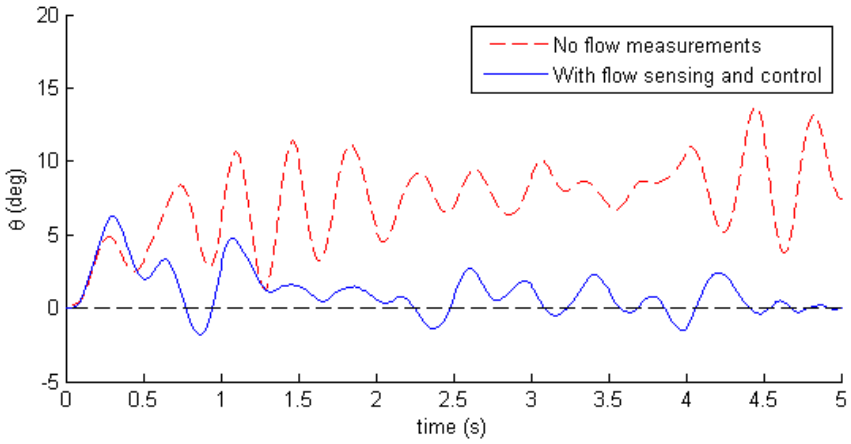

(a): Pitch angle history

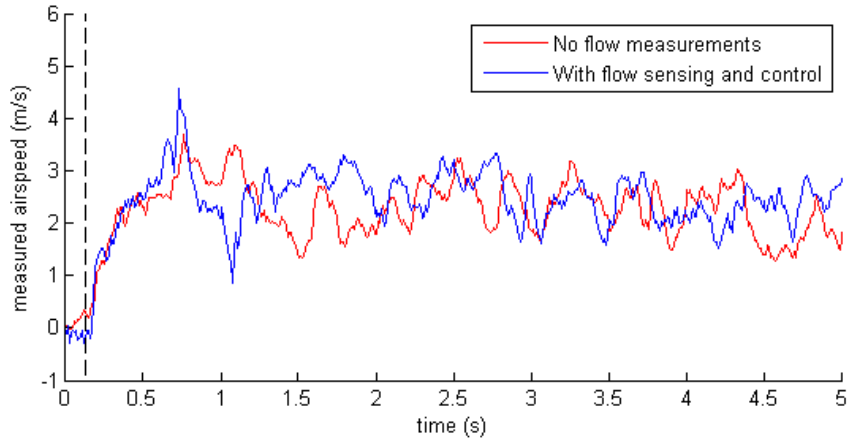

(b): Onboard flow measurements

Figure 8: Experimental results from a 0m/s to 2.5m/s freestream increase

In both cases, the system responds to the step increase in freestream velocity by rotating away from the flow. Without the feedback linearization scheme, the system experiences a number of pitch oscillations before settling into a steady state error of approximately 7° in the new flow conditions. With flow feedback control enabled, the test stand undergoes fewer oscillations and is able to more closely track the reference pitch angle.

Table 1: Table of relevant parameters

Parameter	Simulation	Experiment
$\Omega\ (rad/s)$	400	390
$\nu\ (m/s)$	2.5	2.5
$l\ (m)$	0.12	0.12
$d\ (m)$	0.02	0.02
$I\ (kgm^2)$	2.1 e^{-4}	2.1 e^{-4}
$k_f\ (ms)^{-1}$	2.2 e^{-3}	N/A
$k_S\ (kg)$	2.03 e^{-6}	N/A
$k_S k_f\ (kg)$	4.46 e^{-9}	4.46 e^{-9}
$k_T^{(1)}\ (kgm)$	1.1 e^{-6}	1.1 e^{-6}
$k_T^{(2)}\ (kgm^{-1})$	1.05 e^{-5}	1.05 e^{-5}

V. Conclusion and Ongoing Work

A single-degree-of-freedom dynamic model that includes the aerodynamic effects of an edgewise free-stream on a rotor has been built and tested. Onboard flow measurements are used to feedback linearize the system. Data from a series of rotor tests support the implementation of the control strategy with small quadcopter rotors. Experimental results from a tandem-rotor pitch stand in constant and varying flow conditions are presented, demonstrating the potential advantage of onboard flow feedback for attitude control in wind. Ongoing work seeks to develop measurement filtering techniques and explore turbulence mitigation.

References

[1]M. Belkheri, A. Rabhi, A. Hajjaji, and C. Pergard. Different linearization control techniques for a quadrotor system. In *2nd Int. Conf. on Communications, Computing and Control Applications,*, pages 1–6, December 2010.

[2]D. Alexander and S. Vogel. *Nature's Flyers: Birds, Insects, and the Biomechanics of Flight.* Johns Hopkins University Press, October 2004.

[3]R. Brown and M. Fedde. Airflow sensors in the avian wing. In *Journal of Experimental Biology*, volume 179, pages 13–30, 1993.

[4]S. Herwitz, K. Allmendinger, R. Slye, S. Dunagan, B. Lobitz, L. Johnson, and J. Brass. Nighttime UAV vineyard mission: Challenges of see-and-avoid in the NAS. In *Proc. AIAA 3rd Unmanned Unlimited Conference, Workshop and Exhibit*, pages 1–6, September 2004.

[5]R. Beard, D. Kingston, M. Quigley, D. Snyder, R. Christiansen, W. Johnson, T. McLain, and M. Goodrich. Autonomous vehicle technologies for small fixed wing UAVs. In *AIAA Journal of Aerospace Computing, Information, and Communication*, volume 2, page 92, January 2005.

[6]R. Hirokawa, D. Kubo, S. Suzuki, J. Meguro, and T. Suzuki. Small UAV for immediate hazard map generation. In *AIAA Infotech@Aerospace Conf*, May 2007.

[7]A. Mohamed, M. Abdulrahim, S. Watkins, and R. Clothier. Development and flight testing of a turbulence mitigation system for micro air vehicles. In *Journal of Field Robotics*, August 2015.

[8]F. Hsiao, Y. Ding, C. Chuang, C. Lin, and Y. Huang. The design of a small UAV system as a testbed of formation flight. In *AIAA Infotech@Aerospace Conf*, March 2011.

[9]N. Rasmussen, B. Morse, and C. Taylor. Fixed-wing, mini-UAV system for aerial search operations. In *AIAA Guidance Navigation and Control Conference and Exhibit*, August 2007.

[10]P. Xie, A. Flores-Abad, G. Martinez, and O. Ma. Development of a small UAV with autopilot capability. In *Proc. AIAA Atmospheric Flight Mechanics Conference*, August 2011.

[11]C. Hall. C. Cox, A. Gopalarathnam. Flight test of stable automated cruise flap for an adaptive wing aircraft. In *Journal of Aircraft,*, volume 47, pages 1178–1188, January 2009.

[12]D. Yeo, E. Atkins, L. Bernal, and W. Shyy. Aerodynamic sensing for a fixed wing uas operating at high angles of attack. In *Proc. AIAA Atmospheric Flight Mechanics Conference*, August 2012.

[13]D. Yeo, N. Sydney, D. Paley, and D. Sofge. Onboard flow sensing for downwash detection and avoidance with a small quadrotor helicopter. In *Proc. AIAA Guidance Navigation and Control Conference*, January 2015.

[14]M. Patel, Z. Sowle, T. Corke, and C. He. Autonomous sensing and control of wing stall using a smart plasma slat. In *Proc. 44th AIAA Aerospace Sciences Meeting*, January 2006.

[15]P.Bowles and T. Corke. Stall detection on a leading-edge plasma actuated pitching airfoil utiliizing onboard measurement. In *Proc. 47th Aerospace Sciences Meeting*, January 2009.

[16]W. Barnwell. Flight Control Using Distributed Actuation and Sensing. Master's thesis, North Carolina State University, Raleigh, NC, USA, 2003.

[17]N. Sydney, B. Smyth, and D. A. Paley. Dynamic control of autonomous quadrotor flight in an estimated wind field. In *Decision and Control (CDC), 2013 IEEE 52nd Annual Conference on*, pages 3609–3616, Dec 2013.

[18]J. G. Leishman. *Principles of Helicopter Aerodynamics*. Cambridge University Press, April 2006.

[19]R. W. Prouty. *Helicopter Performance, Stability, and Control*. Krieger Publishing Company, 2002.

[20]D. Mellinger and V. Kumar. Minimum snap trajectory generation and control for quadrotors. In *IEEE International Conference on Robotics and Automation*, May 2011.

[21]E. de Vries and K. Subbarao. Backstepping based nested multi-loop control laws for a quadrotor. In *11th Conference on Control Automation Robotics Vision*, December 2010.

[22]G. Fiore J. P. How M. Valenti, B. Bethke and E. Feron. Indoor multi-vehicle flight testbed for fault detection, isolation, and recovery. In *Proc. AIAA Guidance Navigation and Control Conference*, August 2006.

[23]S. Waslander G. Hoffman, H. Huang and C. Tomlin. Quadrotor helicopter flight dynamics and control: Theory and experiment. In *Proc. AIAA Guidance Navigation and Control Conference*, August 2007.

[24]S. Waslander H. Huang, G. Hoffman and C. Tomlin. Aerodynamics and control of autonomous quadrotor helicopters in aggressive maneuvering. In *IEEE International Conference on Robotics and Automation*, May 2009.

[25]S. Waslander G. Hoffman, H. Huang and C. Tomlin. Precision flight control for a multi-vehicle quadrotor helicopter testbed. In *Control engineering practice*, volume 19, pages 1023–1036, January 2011.

[26]J. Gresham P. Corke J. P. Pounds, R. Mahony and Roberts. Towards dynamically-favourable quad-rotor aerial robots. In *Australasian Conference on Robotics and Automation*, 2004.

[27]D. J. Salmond N. J. Gordon and A. F. Smith. Experimental model predictive attitude tracking control of a quadrotor helicopter subject to wind-gusts. In *Radar and signal Processing*, volume 140, pages 107 –113, 1993.